RSC Advances

PAPER

View Article Online
View Journal | View Issue

Cite this: *RSC Adv.*, 2025, **15**, 37990

Optimization and characterization of a castor oil (*Ricinus communis* L.)- and 1,10-phenanthroline-based polyurethane membrane for Al^{3+} ion-selective applications

Eka Safitri, *[a] Nazaruddin Nazaruddin,[a] Dalia Qurrattu Aini,[a] Muhammad Ridho Afifi,[a] Khairi Suhud,[a] Faizatul Shimal Mehamod,[b] Sagir Alva,[c] Rinawati,[d] Nurul Hidayat,[e] Cut Nanda Nurbadriani[f] and Muhammad Jurej Alhamdi[g]

Received 23rd June 2025
Accepted 17th September 2025

DOI: 10.1039/d5ra04455c

rsc.li/rsc-advances

Ion-selective membrane technology is a key for accurately measuring specific ions in different solutions. A study on Al^{3+} ion selective electrodes (ISEs) based on polyurethane (PU) membranes using an active substance, *i.e.*, 1,10-phenanthroline, was successfully conducted. The results showed the highest sensitivity and linear range with a PU membrane composition of castor oil, toluene diisocyanate, 1,10-phenanthroline, and acetone in the ratio of 37.80 : 18.90 : 43.20 : 0.10 (%w/w) and internal solution composition 0.1 : 0.1 (M) of KCl and $Al(NO_3)_3$ Fourier transform infrared (FTIR) analysis indicated the presence of urethane bonds at a wavenumber of 3390 cm^{-1}. 1,10-Phenanthroline aromatic C=C and C–N functional group peaks appeared at wavenumbers of 1600 cm^{-1} and 1325 cm^{-1}, respectively. X-ray diffraction (XRD) characterization suggested a decrease in the degree of crystallinity of PU, PU/Phen membranes, and PU/Phen/Al. Scanning electron microscopy (SEM) analysis showed that the PU/Phen/Al membrane had a homogeneous dense outer layer and tended to be porous in the inner layer, and the Al^{3+} ISE system showed an average sensitivity, linear range, and detection limit of 19.94 ± 0.26 mV/decade, 10^{-10}–10^{-4} M (R^2 = 0.998), and 5.17 × 10^{-12} M, respectively. Furthermore, the ISE had a response time of 180 s, was stable in the pH range of 6–8 and allowed 33 days of use without any interference from foreign ions. The recovery was in the range of 99.21–101.57%. Therefore, the prepared PU/Phen/Al membrane is promising for ISE sensors, especially for the detection of Al^{3+} ions.

Introduction

Aluminum (Al) is a significant environmental pollutant due to the disposal activities associated with metal coating industries. Exposure to Al metal at high concentrations over a prolonged period can cause poisoning, allergies, and metabolic disorders in human.[1] Therefore, it is critical to develop an accurate, fast, simple, and cheap detection system to mitigate these ongoing negative impacts. Until now, several methods have been used to detect Al, such as atomic absorption spectroscopy (AAS), X-ray fluorescence (XRF), and inductively coupled plasma mass spectrometry (ICP-MS).[2–4] However, these instruments are expensive and require trained operators.

Current developments in analytical techniques have shifted towards simpler methods with higher accuracy. One such recently developed technique is potentiometry which uses ion-selective electrodes (ISEs) and ion-selective field-effect transistors (ISFETs) selectively target ions in samples.[5,6] These potentiometric devices can be used for portable measurement[7] and have been applied to analyze industrial, medical, and environmental samples.[8]

The membrane's selectivity is determined by the active substance's affinity for the target analyte to selectively recognize and bind the analyte. Various membranes have been reported as matrices, for example, polyvinyl chloride (PVC).[9,10] Several Al^{3+} ISEs based on PVC membranes have been reported using active ingredients such as tetradentate Schiff bases,[11] neutral carrier morin,[12] 5,10,15,20-tetrakis(*p*-chlorophenyl)porphyrin,[13] and 12-crown-4 as an ionophore.[14] However, PVC membranes

[a]*Department of Chemistry, Faculty of Mathematics and Natural Sciences, Universitas Syiah Kuala, Banda Aceh 23111, Indonesia. E-mail: e.safitri@usk.ac.id*
[b]*Advanced Nano Materials (ANoMa) Research Group, Faculty of Science and Marine Environment, Universiti Malaysia Terengganu, 21030 Kuala Nerus, Terengganu, Malaysia*
[c]*Mechanical Engineering Department, Faculty of Engineering, Universitas Mercu Buana, West Jakarta, Indonesia*
[d]*Department of Chemistry, Faculty of Mathematics and Natural Science, Universitas Lampung, Bandar Lampung, Indonesia*
[e]*Department of Physics, Faculty of Mathematics and Natural Sciences, Universitas Negeri Malang, Malang, Indonesia*
[f]*Department of Electrical and Computer Engineering, Universitas Syiah Kuala, Banda Aceh, Indonesia*
[g]*PT PLN (Persero), Makassar System Load Dispatch Center, Indonesia*

have disadvantages, including their rigid nature and the need for plasticizers and lipophilic salts to make them plastic and charged.[15]

The membrane is crucial for ISE construction because it serves as a binding matrix for active substances to produce a selective membrane. Polyurethane (PU) membranes are known for their excellent mechanical strength and unique chemical properties.[16–18] The available NH and C=O functional groups provide a negative membrane characteristic,[19] and therefore, PU membranes can act as cation-selective membranes. Due to their intrinsic flexibility, PU membranes obviate the need for external plasticizers or lipophilic additives, which are typically employed to enhance membrane pliability. Some works have reported the use of PU membranes as an ion-selective sensor matrix.[20,21]

Several researchers reported ISE construction based on PU membranes modified with 1,10-phenanthroline to produce ion-selective membranes for detecting Cr^{3+} ions[20] and Pb^{2+} ions.[21] In this study, a PU membrane was modified using the 1,10-phenanthroline compound with a lone pair of electrons,[22] which formed a complex with Al^{3+} metal ions. The ISE featured an asymmetrical membrane and used an internal solution, with the 1,10-phenanthroline compound known for its ability to form complexes with other metal ions. The internal solution of the ISE working system could stabilize the electrode and enhance the selectivity towards Al^{3+} ions.

Experimental methods

Materials

Materials used in this research included 1,10-phenanthroline, $Pb(NO_3)_2$, acetone, toluene diisocyanate (TDI), KCl, $FeCl_3$, $NaNO_3$, $Cr(NO_3)_3$, $CuSO_4$, $ZnSO_4$, $Cd(NO_3)_2$, $Ni(NO_3)_2$, $Co(NO_3)_2$, $Mg(NO_3)_2$, KNO_3, $Fe(NO_3)_3$, $FeCl_3$, CH_3COOLi, and a Ag wire. All the aforementioned chemicals were purchased from Merck in analytical grade quality. Commercial castor oil (*Ricinus communis* L.) was procured from PT. Rudang Jaya (Medan, Indonesia) in industrial grade quality and agar was purchased from trademark Akos.

Instruments

Instruments for the prepared membranes characterizations were a scanning electron microscope (SEM) with the serial name JEOL JSM 6360 LA (Tokyo, Japan), an X-ray diffractometer (XRD) (Shimadzu XRD-700 Series, Kyoto, Japan), a Fourier transform infrared (FT-IR) spectrometer (Shimadzu Prestige, Kyoto, Japan), and a universal testing machine HT8503 (Hung Ta Instrument Co., Ltd, Taichung, Taiwan). In addition, the analytical performance of the Al^{3+} ISE was evaluated using a Thermo Orion Scientific Star A211 potentiometer (Waltham, MA, USA).

1,10-Phenanthroline-modified polyurethane membrane preparation

The polyurethane membrane was prepared by reacting 3.5 grams of commercial castor oil (*Ricinus communis* L.) with 1,10-phenanthroline in various compositions (see Table S1). The mixed composition was stirred for 24 hours until dissolved. Next, it was reacted with 1.75 grams of TDI by heating at 60 °C for 15 minutes. The resulting dope solution was yellowish in color and added with ±4 grams of acetone printed on a glass surface 25 cm × 15 cm with a thickness of 0.5 mm and dried for 24 hours at 60 °C to produce thin layered membranes. The Al^{3+} ISE was constructed by cutting a PU membrane with a diameter of 1.3 cm and putting it properly on the bottom of the electrode. The ISE internal solutions contained 0.1 M KCl and 0.1 M $Al(NO_3)_3$. The composition of the internal solution was varied (see Table S2) to obtain the optimum ISE response.

Fig. 1 Fabricated electrodes in a potentiometer.

Study of Al^{3+} ISE performances

Nernst factor, linear range, LOD, and LOQ determination. The measurement potential was determined using a Thermo Orion Start A211 potentiometer and Ag/AgCl as a reference electrode. Fig. 1 shows the fabricated electrodes in the instrument potentiometer. A plot of the potential *versus* Al^{3+} concentration in standard solutions of 10^{-10}–10^{-1} M was used to determine the ISE sensitivity, linear range, limit of detection (LOD), and limit of quantification (LOQ). 0.1 M $NaNO_3$ was used as a blank solution to determine the LOD and LOQ, which were calculated according to eqn (1) and (2), respectively. The Y_{LOD} and Y_{LOQ} values were then used to calculate the LOD and LOQ from the linear range equation of the calibration curve.

$$Y_{LOD} = \text{average blank} + 3SD \quad (1)$$

$$Y_{LOQ} = \text{average blank} + 10SD \quad (2)$$

Response time. The Al^{3+} ISE response time was determined based on the time needed to obtain a stable response for measuring a series of Al^{3+} standard solutions of 10^{-10}–10^{-1} M.

Effect of the pH. The resistance of the Al^{3+} ISE to pH was determined using a 10^{-3} M $Al(NO_3)_3$ solution dissolved in various phosphate buffers with pH values of 4, 5, 6, 7, 8, and 9. The effect of the solution pH on the potential response was determined by plotting the pH against the potential values.

ISE lifetime. A study on the Al^{3+} ISE lifetime was carried out by measuring the potential of a series of standard solutions of $Al(NO_3)_3$ with concentrations of 10^{-10}–10^{-1} M. The potential measurement of the 10^{-10}–10^{-1} M $Al(NO_3)_3$ solutions was performed using a similar procedure on days 10, 15, 20, 25, and 30. A graph of the potential value (mV) *versus* the −log Al^{3+} concentration was used for the assessment of the changes in the ISE sensitivity, dynamic range, and R^2 values on different days.

Selectivity coefficient. Determination of the Al^{3+} ISE was conducted to determine its ability to respond to Al^{3+} ions and various foreign ions with valences I, II, and III. The determination of the ISE selectivity was conducted using a separate method, and the ions tested were K^+, Li^+, Na^+, Ni^{2+}, Mg^{2+}, Ca^{2+}, Co^{2+}, Cd^{2+}, Cu^{2+}, Zn^{2+}, Pb^{2+}, Fe^{3+}, and Cr^{3+}. The concentration of foreign ions used in this study was 10^{-4} M, and eqn (3) was used to calculate the selectivity coefficient.

$$K_{ij} = \frac{10^{\Delta E/S} \times a_i}{a_j^{z_i/z_j}} \quad (3)$$

A separate solution method was carried out by measuring the Al^{3+} and interfering ion solutions separately. The selectivity coefficient was then determined using eqn (3).

Results and discussion

Polyurethane characterizations

The functional group, crystalline properties, and surface morphologies of polyurethane membranes modified with 1,10-phenanthroline were characterized using Fourier transform infrared (FTIR) spectroscopy, X-ray diffraction (XRD) and scanning electron microscopy (SEM), respectively.

Functional group analysis of polyurethane membranes. The reaction between alcohol (–OH) and isocyanate produced PU membranes *via* urethane bonds.[18] The PU membrane was synthesized using different compositions of castor oil, 1,10-phenanthroline, and TDI (Table S1) to obtain a suitable PU characteristic as a sensor matrix. The proper membrane was thin and plastic. Fig. 2 shows the FTIR spectra of the prepared membranes.

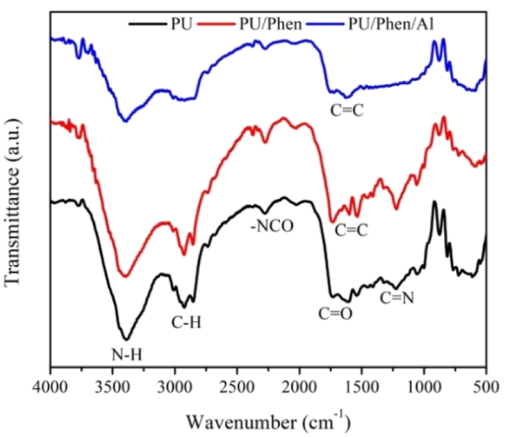

Fig. 2 FTIR spectra of PU, PU/Phen, and PU/Phen/Al membranes.

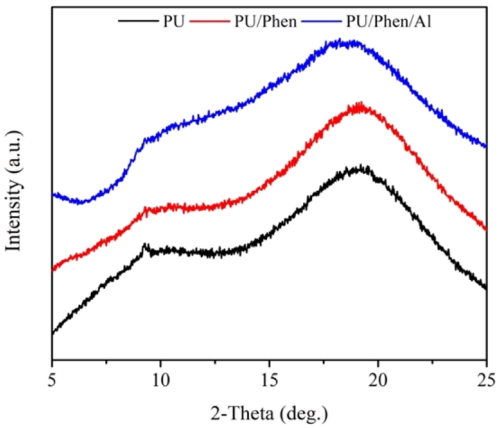

Fig. 3 XRD patterns of PU, PU/Phen, and PU/Phen/Al membranes.

The PU membrane characterization results showed FTIR peaks at several wavenumbers, such as the typical absorption at a wavenumber of 3390 cm^{-1} indicated the absorption of the –NH group of urethane.[23] The absorption at wavenumbers of 2924 cm^{-1} and 2852 cm^{-1} indicated the presence of the –CH group. Meanwhile, the absorptions at wavenumbers of 1323 cm^{-1} and 1600 cm^{-1} indicated the existence of the C–N functional group. The weakening of the –NCO absorption from 2,4-toluene diisocyanate (TDI) was observed at 2277 cm^{-1}.[23] The presence of 1,10-phenanthroline in the modified membrane was indicated by a peak at a wavenumber of 1535 cm^{-1}.

The PU membrane modified using 1,10-phenanthroline was characterized by a peak at a wavenumber of 1535 cm^{-1}, associated with the presence of the aromatic group –C=C from 1,10-phenanthroline. Furthermore, the –C–N group was marked by a peak at a wavenumber of 1325 cm^{-1}. Another study[24] observed the –C–N peak in the wavenumber range from 1222 cm^{-1} to 1058 cm^{-1}. The interaction of the PU/Phen membrane with Al^{3+} ions was shown by a shift in the absorption of the aromatic framework at wavenumbers of 1485 cm^{-1}, 1440 cm^{-1}, and 1409 cm^{-1}. This indicated the interaction of Al^{3+} ions with the aromatic nitrogen-containing rings of 1,10-phenanthroline.

Crystal structure analysis of polyurethane membranes

Polyurethane is a polymer containing urethane functional groups in its molecular chain. PU and its modifications are partially crystalline. The crystallinity of the membranes was investigated by XRD analysis. The XRD pattern can also provide information about the chain configuration in the crystalline, the estimated crystalline size, and the comparison of crystalline areas with amorphous areas (the degree of crystallinity). These structural properties influence the performance of the PU membrane.[17]

Table 1 Crystallinity of the PU-based membranes

No.	Membrane	Crystallinity (%)
1	PU	4.03
2	PU/Phen	2.60
3	PU/Phen/Al	2.49

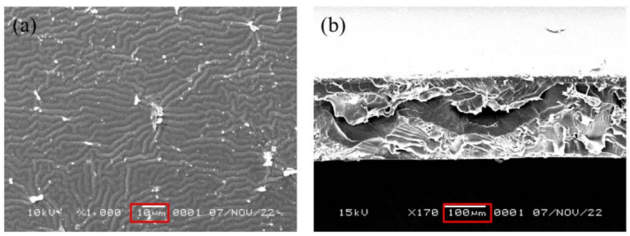

Fig. 4 SEM images of the PU/Phe/Al membrane captured from the (a) top and (b) cross-section.

According to the XRD data depicted in Fig. 3, the prepared PU, PU/Phen, and PU/Phen/Al membranes exhibited semi-crystalline characteristics. The degrees of crystallinity of the three types of membranes are shown in Table 1. The crystallinity degree of the PU membrane was modified using 1.10-phenanthroline and aluminum. The presence of added materials decreased the crystallinity, implying that they made the structure more flexible to carry out the diffusion process. By contrast, the degree of crystallinity has a significant correlation with the glass transition (T_g) value. As the crystallinity decreases, the glass transition also decreases.[25] The presence of 1,10-phenanthroline caused a decrease in the crystalline degree by 55%, with an additional 4.33% reduction when the PU/Phen membrane interacted with Al^{3+} ions.

The decrease in the crystallinity of the modified membranes facilitated the diffusion process, making them beneficial for Al^{3+} ion-selective sensing purposes. The relationship between diffusion and the decreasing degree of crystallinity has also been reported by Trifol *et al.*[26] The XRD patterns of PU, PU/Phen, and PU/Phen/Al membranes had broadening peaks at 19.02°, 19.33° and 18.91°.

Morphological characteristics of the PU/Phen/Al membrane

SEM images were captured to monitor the morphological properties of the PU/Phen/Al membrane, as provided in Fig. 4. The result of the cross-sectional analysis showed that the modified PU membrane had outer and inner layers. The top layer was solid, followed by a hollow categorized as an asymmetric membrane. This result was consistent with other studies.[20,21] A dense layer on the outer surface is advantageous for sensor membrane applications, as it prevent leaks, which are a potential cause of an unstable response.

Optimization of the membrane composition

The working system for ion-selective electrodes requires a matrix that influences selectivity, stability, and mass transport. Meanwhile, the mechanical properties and thermal stability determine the lifespan of the ISE.[27] Then, a 1,10-phenanthroline-modified polyurethane membrane was used as the active substance for ISE selectivity towards Al^{3+} ions.

The membrane is crucial in the ISE working system's functioning for active substance immobilization. The matrix and stability of the ISE have a significant correlation with its sensitivity and lifetime. In this situation, the quantity of ionophores in the membrane affects the stability and sensitivity. After use, the decrease in sensitivity might be due to the leaching process and the insufficient amount of ionophores. The close sensitivity value to the theoretical Nernst factor (19.72 mV/decade) of the value of 3-valent metals was 18.90 mV/decade with the widest dynamic range. The influence of the membrane composition on the sensitivity and linear range is shown in Table S3.

Table S3 presents that the optimum membrane composition for achieving sensitivity close to the theoretical value was castor oil : TDI : 1,10-phenanthroline : acetone in the ratio of 37.80% : 18.90% : 0.10% : 43.20% (w/w). 10 mg of 1,10-phenanthroline was appropriate for the creation of attractive forces between 1,10-phenanthroline in the membrane and Al^{3+} ions in the external solution. During the measurement process, the ion exchange occurred between the aluminum bound to the membrane and the Al^{3+} ions in the solution to reach an equilibrium state.

When equilibrium was reached, the difference in charge density formed a potential difference on the surface of the ISE membrane. The potential value was proportional to the activity of Al^{3+} ions in the solution. However, the presence of NO_3^- in the standard solution created a repulsive force on the membrane surface due to the similarity of the charge between the membrane and the NO^{3-} ions. Therefore, NO^{3-} ions moved away from the membrane surface, according to Le Chatelier's principle.[21,28] During equilibrium, as determined by Le Chatelier's principle, the diffusion process occurred from a region with a high Al^{3+} ion concentration to the one with a low concentration. This depended on the availability of Al^{3+} ions (inside or outside the membrane).

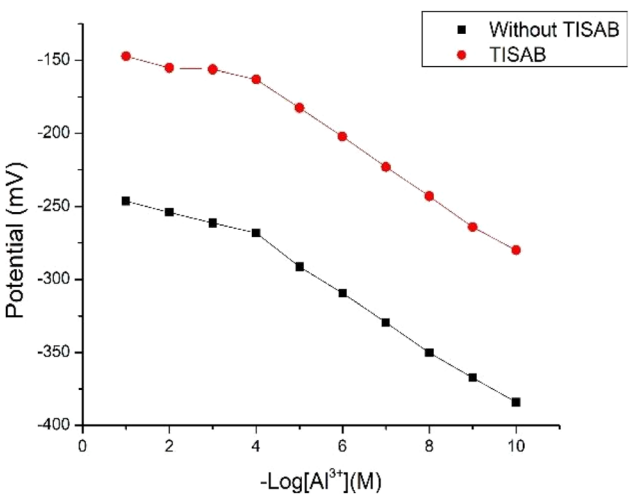

Fig. 5 ISE responses with TISAB and without TISAB solutions.

Table S3 shows that the highest sensitivity achieved was 19.86 ± 0.34 mV/decade. The increased concentration of 1,10-phenanthroline appears to enhance sensitivity, likely due to strengthened coulombic interactions between the ionophore and the target ion. This enhancement may also be attributed to the increased availability of active binding sites, which promotes a greater concentration gradient at the membrane–solution interface. Consequently, ion flux across the membrane is enhanced, leading to a more pronounced potential difference, often observed as an overpotential response. However, an excessive amount of the ionophore may cause a super-Nernstian response, likely due to an imbalance between the ionophore concentration and the availability of target ions, as previously reported.[29] While such conditions may temporarily improve detection capabilities, sensitivity values closer to the theoretical Nernstian slope are generally preferred to ensure analytical stability and reliability.

Optimization of the internal solution composition

The optimization of the internal solution composition was performed to evaluate its effect on the ISE sensitivity. The internal solution consisted 0.1 M KCl and various $Al(NO_3)$ concentrations aimed to stabilize the electrode response. The conventional ISE working system uses an internal solution. Therefore, the difference in the charge density on the two membrane interfaces forms a proportional potential to the Al^{3+} ion activity in the analyte solution, and in this situation, the two sides of the membrane interface produce a boundary phase potential. A similar consequence was also stated by Mohan *et al.*[27] In other experiments, we found that the changes in sensitivity were affected by a difference in the internal solution activity.[21] The $Al(NO_3)_3$ concentrations used were 0, 0.1, 0.3, 0.5, and 0.7 M. The sensitivity values (mV per decade) for various variations are presented in Table S4.

Table S4 shows the effect of the internal solution composition on the ISE sensitivity and linear range. The higher concentration of the $Al(NO_3)_3$ solution caused an increase in sensitivity, and a significant increase occurred when the internal solution contained $Al(NO_3)_3$ compared to one without $Al(NO_3)_3$ solutions. As shown in Table S4, the $Al(NO_3)_3$ concentrations of 0.3, 0.5, and 0.7 M increased the sensitivity, but the linear ranges were narrow. This might be due to the presence of more Al^{3+} ions on the inner side than on the outer side. Therefore, the difference in the potential between them was negligible. According to Table S4, the optimum internal solution concentration was achieved at 0.1 M $Al(NO_3)_3$ and 0.1 M KCl solutions.

Effect of the total ionic strength-adjuster buffer

The ISE performance is also influenced by the ionic strength. Therefore, the influence of the total ionic strength adjuster buffer (TISAB) on the measurement of standard solutions containing TISAB needs to be studied. The TISAB solution used in this study was 10^{-3} M $NaNO_3$. The ISE response profiles of Al^{3+} to standard solutions containing TISAB and without TISAB are shown in Table S5.

Fig. 5 shows the ISE responses to TISAB solution addition. It indicated that the presence of the TISAB solution did not significantly affect sensitivity but did influence the dynamic range. The measurement results showed that the TISAB solution affected the Al^{3+} ISE potential, resulting in a change in the linear range of measurement from 10^{-9}–10^{-4} M to 10^{-10}–10^{-4} M. The TISAB solution could stabilize ionic strength at low concentrations.[21]

Determination of ISE performance

The quality of the Al^{3+} ISE is determined by the Nernst factor, linear range, limit of detection, response time, lifetime, effect of pH, selectivity, reproducibility, repeatability, and percent recovery. The Al^{3+} ISE performance was determined using the optimum membrane composition (%w/w) of castor oil : TDI : 1,10-phenanthroline : acetone (37.80 : 18.90 : 0.10 : 43.20) and an internal solution (0.1 M $Al(NO_3)_3$ + 0.1 M KCl). The measurement was performed using a series of standard solutions of $Al(NO_3)_3$ with concentrations of 10^{-10}–10^{-1} M containing a TISAB solution of 10^{-3} M $NaNO_3$. Al^{3+} ISE conditioning was carried out by immersing it in a 0.1 M $Al(NO_3)_3$ solution for ±24 hours.

Sensitivity and linear range. The Nernst factor and linear range were determined by measuring the ISE potential of Al^{3+} against a series of standard solutions containing $Al(NO_3)_3$ with a concentration of 10^{-10}–10^{-1} M. Measurements started from the dilute to the highest concentration solutions. The potential (mV) was plotted against $-\log [Al^{3+}]$ (M) at various concentrations. The Nernst factor and linear range are provided in Table 2.

Table 2 shows the optimum Al^{3+} ISE that produces an average sensitivity of 19.94 ± 0.26 mV/decade with a linear concentration range of 10^{-10}–10^{-4} M. This value was close to the theoretical value for trivalent ions (19.73 mV/decade). The difference in sensitivity values for each ISE might be because the dispersion of 1,10-phenanthroline was not homogeneous, and standard deviations were below 5%. Therefore, the measurement had an acceptable precision value. The resulting potential profile increases with increasing concentration, which is responsible for the Al^{3+} ISE, described by eqn (1).

$$E_{sel} = E^{\circ}_{sel} + s \log[Al^{3+}] \quad (4)$$

where s is the slope value associated with a theoretical sensitivity of 19.73 mV per decade) for ISE analytes with valence 3.

Table 2 Al^{3+} ISE sensitivity and linear range

ISE	I	II	III	IV	V
Sensitivity (mV/decade)	19.48	20.23	19.61	20.11	20.04
Linear range (M)	10^{-10}–10^{-4}	10^{-10}–10^{-4}	10^{-10}–10^{-4}	10^{-10}–10^{-4}	10^{-10}–10^{-4}
Determination coefficient (R^2)	0.999	0.995	0.996	0.990	0.999

The linear range was determined based on the linear potential response to the $Al(NO_3)_3$ standard solution, and the results obtained in this study were in the range of 10^{-10}–10^{-4} M. The non-linear Al^{3+} ISE measurement showed the inability of the ISE to stimulate potential changes on the electrode surface,[28] which occurred at the lowest and highest concentrations of the standard solution. In this study, the Al^{3+} ISE was unable to respond to potential changes in the concentration ranges of 10^{-3}–10^{-1} M and 10^{-13}–10^{-11} M.

Limit of detection. The limit of detection (LOD) was determined to obtain the lowest concentration limit for the detection of Al^{3+} ions. In the ISE working system, the detection limit is affected by the type of ionophore and membrane. In this study, the LOD was also determined by measuring the blank potential of 10^{-3} M $NaNO_3$ as a blank solution; therefore, the Y_{LOD} was obtained through eqn (5).

$$Y_{LOD} = 3 \times \text{STDV blank} + \text{potential} \quad (5)$$

The results obtained were then used to obtain XLOD = 5.17×10^{-12} M through the linear calibration curve equation, and the Al^{3+} ISE limit of quantitation (LOQ) value was 6.8×10^{-12} M. The LOD value obtained in this study is better than that in the research reported by Jannah *et al.*[30]

Response time. The Al^{3+} ISE's response time was determined based on an equilibrium point at the membrane interface to achieve a stable potential. The determination of response time was performed using three $Al(NO_3)_3$ concentrations, namely, 10^{-4}, 10^{-7}, and 10^{-10} M. The response time produced in the measurement is shown in Fig. 6.

The measurement shows that the average response time was stable after 180 seconds of measurement, with a change of 0.07 mV in the potential. This was because the equilibrium at the membrane interface had not been achieved yet. Then, the stability in potential is also influenced by the concentration and the presence of interfering ions in the solution. It normally occurs in a fast, stable response at higher concentrations. The response time is also affected by the impedance of the membrane.[31–33]

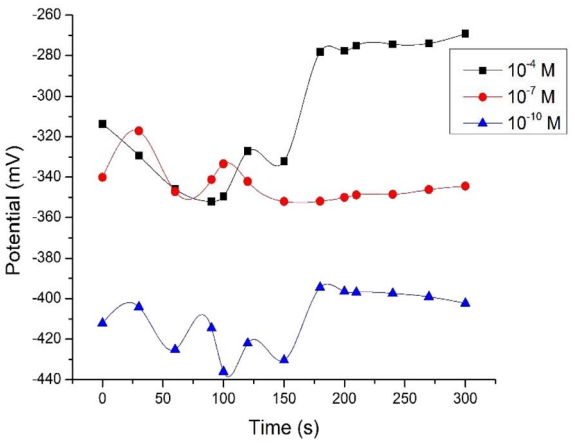

Fig. 6 Al^{3+} ISE response time curve.

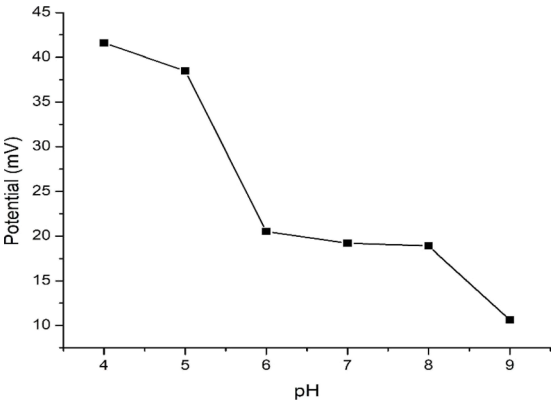

Fig. 7 The profile of the Al^{3+} ISE response at different pH values.

Effect of pH. A study of the pH effect on the potential ISE response to the Al^{3+} ion was needed to determine the robustness at various solution pH values. A good ISE performance is not influenced by pH because the pH in real samples might vary. If the ISE response is affected by the pH, it is necessary to adjust the pH first so that the measurement conditions will be the same. In this study, the effect of pH on the ISE response was investigated using standard solutions of the same concentration at different pH levels (4, 5, 6, 7, 8, and 9) prepared with 0.1 M phosphate buffer, as presented in Fig. 7.

Fig. 7 shows that the ISE's response is affected by acidic (<6) and alkaline (>8) pH. The Al^{3+} ISE provides a stable response in the pH range of 6–8. At low pH, excess H^+ ions cause membrane protonation, resulting in competition for the movement of H^+ and Al^{3+} ions to the membrane surface. The same thing was also reported by Ali *et al.*[34] The excess positive charge in the solution causes the ISE potential to increase. By contrast, the potential response tends to decrease at pH > 8 due to the low quantity of free Al^{3+} ions, due to the formation of $Al(OH)_3$. The same phenomenon also occurs in the Al^{3+} ISE using PVC membranes.[11,35]

Effect of foreign ions on the selectivity coefficient. The determination of the Al^{3+} ISE selectivity towards various positively charged foreign ions other than Al^{3+} ions was performed using the separate solution method. Selectivity is the indication

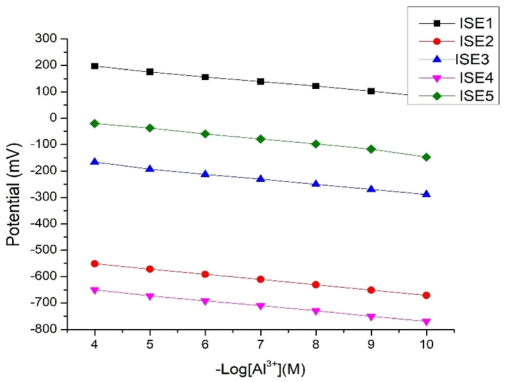

Fig. 8 Al^{3+} ISE reproducibility.

Table 3 Sensing recovery

Sample $-\log[Al(NO_3)_3]$ (M)	ISE $-\log[Al(NO_3)_3]$ (M)	Recovery (%)
4	3.96	99.21
5	5.07	101.57
6	5.96	99.21

of the selectivity coefficient value (K_{ij}) and was tested on several cations with charges I, II, and III (K^+, Zn^{2+}, Mg^{2+}, Pb^{2+}, Fe^{3+}, Co^{2+}, Ni^{2+}, Na^+, Cr^{3+}, and Ca^{2+}) with respective concentrations of 10^{-4} M. Selectivity coefficient calculation results (K_{ij}) are shown in Table S6.

Table S6 shows that the K_{ij} calculation results for the ions tested are <1. The calculation results showed that the Al^{3+} ISE was selective towards Al^{3+} ions compared to foreign ions. The K_{ij} values for foreign ions with valence 3 were higher than those for ions with valences I and II. It can be assumed that trivalent ions, such as Cr^{3+} and Fe^{3+}, possess similar interaction capacities with 1,10-phenanthroline, which consequently leads to selectivity coefficient values being close to 1. Changes in the concentration of the Al^{3+} ion greatly influence the performance of foreign ions. The lower the concentration of the $Al(NO_3)_3$ solution, the more abundant the presence of foreign ions, making them interfere with the measurement process.[36] Based on the calculation results of the foreign ion, the sequence for the Al^{3+} ISE response is $Cr^{3+} > Fe^{3+} > Bi^{2+} > Zn^{2+} > Co^{2+} > Cu^{2+} > Ni^{2+} > Ca^{2+} > Hg^{2+} > Pb^{2+} > Na^+ > K^+ > Li^+$.

ISE lifetime. The lifetime was determined by evaluating the deviation of the Nernst factor value or ISE sensitivity from the theoretical value for trivalent ions (19.73 mV/decade). Further sensitivity deviation indicated a decrease in the ISE sensitivity. The measuring ISE lifetime as shown in Table S7.

Table S7 shows that the decrease in sensitivity occurs gradually as time increases. The same phenomenon also occurs in the Al^{3+} ISE reported in the literature.[35] This might be due to the membrane's swelling during measurement, which caused 1,10-phenanthroline to leach out from the membrane.[21] These data show that the limit of electrode use is the 33rd day, when the sensitivity value obtained is 15.10 ± 0.73 mV/decade, and this value is still acceptable because the lowest sensitivity value for trivalent ions is 14.73 mV/decade. Therefore, day 33 is the limit for the Al^{3+} ISE based on 1,10-phenanthroline-modified polyurethane membranes.

Reproducibility and repeatability. The reproducibility study determines the measurement precision for each ISE under

Table 4 Performance comparison of Al^{3+} ISEs

Material and active compound	Sensitivity mV/decade	Linear range (M)	LOD (M)	Reference
PVC, 7-ethylthio-4-oxa-3-phenyl-2-thioxa-1,2-dihydropyrimido[4,5-*d*] pyrimidine (ETPTP)	19.5	10^{-5}–10^{-1} M	—	37
N,*N*′-Propanediamide bis(2-salicylideneimine) (NPBS)	19.4 ± 0.3	7.9×10^{-7}–1.0×10^{-1}	4.6×10^{-7}	38
Bis(5-phenyl azo salicylaldehyde)2,3-naphthalene diimine (5PHAZOSALNPHN)	19.3 ± 0.8	5.0×10^{-6}–1.0×10^{-2}	2.5×10^{-6}	39
PVC and 6-(4-nitrophenyl)-2-phenyl-4-(thiophen-2-yl)-3,5-diaza-bicyclo[3.1.0]hex-2-ene (NTDH)	19.6 ± 0.4	1.0×10^{-6}–1.0×10^{-1}	1.0×10^{-6}	40
PVC, coated platinum (CPtE), *E*-*N*′-(2-hydroxy-3-methoxybenzylidene) benzohydrazide	19.9 ± 0.3 (PME) and 20.1 ± 0.4 (CPtE)	3.0×10^{-7}–1.0×10^{-2} M for PME and 1.0×10^{-7}–1.0×10^{-2} M for CPtE	$1.7 \times 10(-7)$ and $5.6 \times 10(-8)$ M	41
PVC, 12-crown-4 (12C4)	19.0 ± 0.4	1.0×10^{-6}–1.0×10^{-1}	5.5×10^{-7}	14
(*Z*)-2-(2-Methyl benzylidene)-1-(2,4-dinitrophenyl) hydrazine (L) PVC	20.1 ± 0.5	1.0×10^{-6}–1.0×10^{-1}	10^{-7}	42
1′-[(Methylazanediyl) bis(ethane-2,1-diyl)]-bis[3-(naphthalen-1-yl)thiourea]	17.70 ± 0.13 de	10^{-6}–10^{-2}	2.45×10^{-7}	31
Solid state, neutral carrier morin	8.8	1.0×10^{-5}–1.0×10^{-1}	1.0×10^{-5}	43
Carbon paste, *N*,*N*′-bis(salicylidene)-1,3-propanediamine (SB-Salpr)	20.2 ± 0.1	1.0×10^{-6}–1.0×10^{-2}	2.1×10^{-7}	44
Polyurethane, 1,10-phenantroline and graphene	19.94 ± 0.26	10^{-10}–10^{-4}	5.17×10^{-12}	Present work

similar experimental conditions.[21] The reproducibility study was performed using five electrodes, as shown in Table S8 and Fig. 8.

Table S8 shows that the five Al^{3+} ISEs exhibited an average sensitivity value of 19.94 mV/decade with an acceptable standard deviation of 0.49. Further evaluation involve assessing repeatability which determine the closeness of measurement values under the same measurement conditions. In this study, repeatability was performed through five measurements, which yielded an average sensitivity of 20.16 mV/decade with a standard deviation of 0.12. The sensitivity, linear range, and linearity for each repetitive measurement are shown in Table S9.

Sensing recovery properties

The recovery study determines the accuracy of the ISE for sample measurement. The accuracy of the ISE was evaluated using artificial samples with standard solutions of known concentrations. Table 3 shows that the recovery percentage of the standard solution with three concentrations ranged from 99.21% to 101.57%. This is considered excellent, as a good recovery percentage is typically within the 90–110% range.

Table 4 presents a comparative analysis of the performance between the developed Al^{3+} ISE and other previously reported Al^{3+} ISEs, focusing on their linear response ranges and detection limits. The results indicate that the developed Al^{3+} ISE exhibits a sensitivity value approaching the theoretical Nernstian slope, along with a wider linear response range and a lower LOD compared to previously developed Cr^{3+} ISEs.

Conclusion

The 1,10-phenanthroline-modified PU could be applied as an Al^{3+} ion-selective membrane embedded in the ISE working system. The ISE had a close to theoretical sensitivity value, a wider linear range, and a low-limit detection. It exhibited a stable potential response after 180 seconds, operated effectively within the pH range of 6–8, and maintained its performance over a lifetime of 33 days. This electrode showed a selectivity coefficient less than unity towards foreign ions tested, in the order of $Cr^{3+} > Fe^{3+} > Bi^{2+} > Zn^{2+} > Co^{2+} > Cu^{2+} > Ni^{2+} > Ca^{2+} > Hg^{2+} > Pb^{2+} > Na^{+} > K^{+} > Li^{+}$. Foreign ions with valence III exhibited $K_{ij} \approx 1$, and these ions had the potential to interfere with measurements. Reproducibility and repeatability studies were performed with a standard deviation of less than 5%.

Author contributions

E. Safitri, N. Nazaruddin, and N. Hidayat conceived the study. E. Safitri, S. Alva and D. Q. Aini designed the experiments. D. Q. Aini and M. R. Afifi conducted the experiments. K. Suhud, F. S. Mehamod, C. N. Nurbadriani, M. J Almahdi, and E. Safitri analyzed and interpreted the data. E. Safitri, N. Hidayat, and M. R. Afifi wrote the manuscript, with input from the rest of the authors.

Conflicts of interest

The authors declare no conflict of interest.

Data availability

The data supporting the findings of this study are available from the corresponding author, Eka Safitri, upon reasonable request.

Supplementary information is available. See DOI: **https://doi.org/10.1039/d5ra04455c**.

Acknowledgements

We would like to acknowledge the financial support from Direktorat Riset, Teknologi, dan Pengabdian kepada Masyarakat, Direktorat Jenderal Pendidikan Tinggi, Riset, dan Teknologi, Kementerian Pendidikan, Kebudayaan, Riset, dan Teknologi, Republic of Indonesia, *via* grant number 168/E5/PG.02.00.PL/2023.

Notes and references

1 R. H. Alasfar and R. J. Isaifan, *Environ. Sci. Pollut. Res.*, 2021, **28**, 44587–44597.
2 M. Lanzinger, S. Kaufmann, M. Schuster and N. P. Ivleva, *Microchem. J.*, 2024, **207**, 111782.
3 S. O. Gundogdu, Y. Aytimur, S. Turhan and A. Sahin, *Int. J. Anal. Chem.*, 2025, **2025**(1), DOI: **10.1155/ianc/2793979**.
4 T. Shao, D. Yang, X. Wang, R. Wang and Q. Yue, *Mikrochim. Acta*, 2024, **191**, 716.
5 G. A. Crespo, *Electrochim. Acta*, 2017, **245**, 1023–1034.
6 M. Duraisamy, M. Thangavel, S. Lalitha, K. Jayaram, S. Kumarganesh, K. Martin Sagayam, B. K. Pandey, D. Pandey and S. K. Sahani, *Eng. Rep.*, 2025, **7**, e70126.
7 R. M. P. da Silva, J. Izquierdo, M. X. Milagre, R. A. Antunes, R. M. Souto and I. Costa, *Electrochim. Acta*, 2022, **415**, 140260.
8 Y. H. Cheong, L. Ge and G. Lisak, *Anal. Chim. Acta*, 2021, **1162**, 338304.
9 K. Rashitova, D. Kirsanov, M. Voznesenskiy and O. Osmolovskaya, *Surf. Interfaces*, 2024, **48**, 104326.
10 K. L. Tsou and Y. T. Cheng, *Sens. Actuators Rep.*, 2023, **5**, 100145.
11 A. Abbaspour, A. R. Esmaeilbeig, A. A. Jarrahpour, B. Khajeh and R. Kia, *Talanta*, 2002, **58**, 397–403.
12 R. M. P. da Silva, J. Izquierdo, M. X. Milagre, R. A. Antunes, R. M. Souto and I. Costa, *Electrochim. Acta*, 2022, **415**, 140260.
13 O. Özbek and Ö. Isildak, *Bull. Mater. Sci.*, 2022, **45**, 1–10.
14 M. Esmaelpourfarkhani, G. H. Rounaghi and M. H. Arbab-Zavar, *J. Braz. Chem. Soc.*, 2015, **26**, 963–969.
15 M. Jozanović, N. Sakač, M. Karnaš and M. Medvidović-Kosanović, *Crit. Rev. Anal. Chem.*, 2021, **51**, 115–137.
16 Y. Song, C. Sun, C. Tian, H. Ming, Y. Wang, W. Liu, N. He, X. He, M. Ding, J. Li, F. Luo, H. Tan and Q. Fu, *Chem. Sci.*, 2022, 5353–5362.

17 J. Fan, X. Liang, W. W. Yu, D. Fu, Y. Yu, H. Liu and J. Zhang, *Eur. Polym. J.*, 2023, **198**, 250100.
18 N. Nasrollahi, M. Yousefpoor, A. Khataee and V. Vatanpour, *J. Ind. Eng. Chem.*, 2022, **116**, 99–119.
19 P. Zhang, P. Huang, H. Sun, J. Ma and B. Li, *Environ. Pollut.*, 2020, **257**, 113525.
20 E. Safitri, N. Nazaruddin, R. Humaira, M. R. Afifi, S. Saleha, N. D. Sani, R. Idroes, A. Ulianas, N. Hidayat, B. Rumhayati and E. Yuhana, *J. Electrochem. Soc.*, 2025, **172**, 013504.
21 K. Nisah, R. Rahmi, M. Ramli, R. Idroes, S. Alva, M. Iqhrammullah and E. Safitri, *Membranes*, 2022, **12**, 987.
22 N. Türkel, *ISRN Anal. Chem.*, 2012, **2012**, 1–5.
23 S. Nurman, S. Saiful, B. Ginting, R. Rahmi and M. Marlina, *Indones. J. Chem.*, 2021, **21**, 932–941.
24 R. Kumar, A. Dvivedi and P. Bhargava, *AIP Conf. Proc.*, 2016, **1728**, 1–6.
25 R. Xie, A. R. Weisen, Y. Lee, M. A. Aplan, A. M. Fenton, A. E. Masucci, F. Kempe, M. Sommer, C. W. Pester, R. H. Colby and E. D. Gomez, *Nat. Commun.*, 2020, **11**, 4–11.
26 J. Trifol, D. Plackett, P. Szabo, A. E. Daugaard and M. Giacinti Baschetti, *ACS Omega*, 2020, **5**, 15362–15369.
27 C. Mohan and V. Kumar, *Int. J. Membr. Sci. Technol.*, 2021, **8**, 76–84.
28 S. Alva, A. Widinugroho, M. Adrian, D. S. Khaerudini, S. E. Pratiwi and A. S. A. Aziz, *J. Electrochem. Soc.*, 2019, **166**, B1513–B1519.
29 M. Miyake, L. D. Chen, G. Pozzi and P. Bühlmann, *Anal. Chem.*, 2012, **84**, 1104–1111.
30 F. Jannah, R. Idroes, N. Nazaruddin, N. Idris, E. Safitri and N. D. Md Sani, *Grimsa J. Sci. Eng. Technol.*, 2023, **1**, 78–85.
31 K. S. Ying, L. Y. Heng, N. I. Hassan and S. A. Hasbullah, *Sensors*, 2020, **20**, 6898.
32 J. Gao, L. Wang, Z. Guo, B. Li, H. Wang, J. Luo, X. Huang and H. Xue, *Chem. Eng. J.*, 2020, **381**, 122778.
33 C. Maccà, *Anal. Chim. Acta*, 2004, **512**, 183–190.
34 T. A. Ali, G. G. Mohamed and A. R. Othman, *Int. J. Electrochem. Sci.*, 2015, **10**, 8041–8057.
35 M. Arvand and S. A. Asadollahzadeh, *Talanta*, 2008, **75**, 1046–1054.
36 E. Bakker, E. Pretsch and P. Bühlmann, *Anal. Chem.*, 2000, **72**, 1127–1133.
37 M. B. Saleh, S. S. M. Hassan, A. A. A. Gaber and N. A. A. Kream, *Anal. Chim. Acta*, 2001, **434**, 247–253.
38 Y.-H. Ma, R. Yuan, Y.-Q. Chai and X.-L. Liu, *Mater. Sci. Eng., C*, 2010, **30**, 209–213.
39 A. Abbaspour, A. R. Esmaeilbeig, A. A. Jarrahpour, B. Khajeh and R. Kia, *Talanta*, 2002, **58**, 397–403.
40 M. Arvand and S. A. Asadollahzadeh, *Talanta*, 2008, **75**, 1046–1054.
41 S. Tajik, M. A. Taher and I. Sheikhshoaie, *J. AOAC Int.*, 2013, **96**, 204–211.
42 F. Mizani, S. Salmanzadeh Ardabili, M. R. Ganjaliab, F. Faridbod, M. Payehghadr and M. Azmoodeh, *Mater. Sci. Eng., C*, 2015, **49**, 861–868.
43 R. M. P. da Silva, J. Izquierdo, M. X. Milagre, R. A. Antunes, R. M. Souto and I. Costa, *Electrochim. Acta*, 2022, **415**, 140260.
44 R. S. Khoshnood, S. Akbari and T. M. Chenarbou, *J. Anal. Chem.*, 2022, **77**, 1057–1061.